LONG SUSTAINMENT OF JT-60U PLASMAS WITH HIGH INTEGRATED PERFORMANCE

Y. KAMADA, A. ISAYAMA, T.OIKAWA, Y. SAKAMOTO, N. HOSOGANE, H. TAKENAGA, Y. KUSAMA, T. FUJITA, S. TAKEJI, T. OZEKI, Y. ISHII, S. TOKUDA, K. USHIGUSA, O. NAITO, S. ISHIDA, Y. KOIDE, T. FUKUDA, T. TAKIZUKA, H. SHIRAI, T. HATAE, THE JT-60 TEAM
Naka Fusion Research Establishment,
Japan Atomic Energy Research Institute,
Naka-machi, Naka-gun, Ibaraki-ken, 311-01, Japan

Abstract

LONG SUSTAINMENT OF JT-60U PLASMAS WITH HIGH INTEGRATED PERFORMANCE

This paper treats the recent development of quasi-steady ELMy high-β_p H-mode discharges with enhanced confinement and high-β stability, where i) long sustainment time, ii) increase in absolute fusion performance and iii) expansion of the discharge regime toward low-q_{95} (~3) are emphasized. After modification to the new W-shaped pumped divertor, a long heating time (9sec) with a high total heating energy input of 203MJ became possible without harmful increase in impurity and particle recycling. In addition, optimization of the pressure profile characterized by the double transport barriers, electron density and / or high triangularity δ enabled us to extend the performances in long pulses ; the DT equivalent fusion gain Q_{DT}^{eq}~0.1 (δ =0.16) was sustained for ~9 sec (~50τ_E, ~10τ_p^*) and Q_{DT}^{eq}~0.16 (δ = 0.3) for 4.5s at I_p=1.5MA. In the latter case, H-factor (=$\tau_E/\tau_E^{ITER89PL}$) ~2.2, β_N~1.9 and β_p~1.6 were sustained with 60-70% of noninductive driven current. In the low q_{95} (~3) region, the β-limit was improved by the high δ (~ 0.46) shape where β_N~2.5-2.7 was sustained for ~3.5s with the collisionality close to that of ITER-FDR plasmas. The sustainable β_N is limited by onset of the low-n resistive modes. The direct measurement of the island width shows the agreement with the neoclassical tearing mode theory. The edge pedestal width Δ–ped in the ELMy phase evolves gradually with increasing T_i at the pedestal shoulder and the saturated width (10-15cm at I_p=1MA) is 2-3 times larger than that in the ELM-free phase. The width Δ-ped is proportional to $(a/R)^{0.5}\rho_{pi}$. The limit of the edge α-parameter increases with increasing δ, which is the main reason of the improved high-β stability in a long pulse by high-δ. The sustainable value of $\beta_N H$ increases with increasing δ.

1. SUSTAINMENT OF HIGH PERFORMANCE

Toward the *simultaneous* achievement of i) high confinement , ii) high β, iii) high bootstrap fraction and iv) high efficiency of heat and particle exhaust in the *steady-state*, discharges have been optimized in JT-60U based mainly on the high-β_p H-mode with q(0)>1. Up to I_p=1MA, an optimized pressure profile with high triangularity δ (=0.35) enabled the favorable integrated performance sustained for 2 s with H-factor~ 2.5 and β_N~3 under full non-inductive current drive

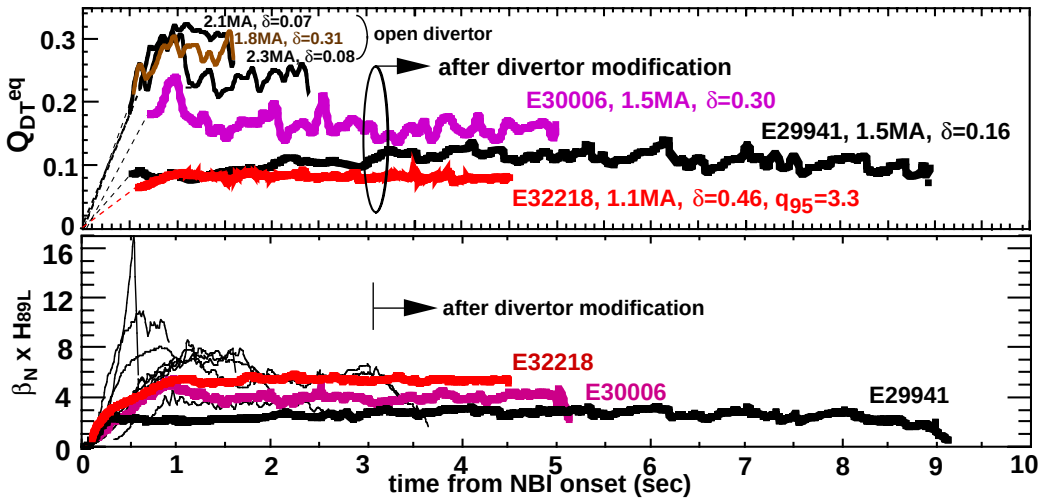

Fig. 1: Sustainment of Q_{DT}^{eq} and $\beta_N H$. Long sustainment became possible with the new divertor.

Table 1: Parameters of long pulse discharges (>10 τ_E) : E29941=' long' , E30006=' high Q' , E32218=' low-q'

shot time(s)	I_p MA	$B_t(0)$ T	κ_x	δ_x	q_{95}	P_{abs} MW	$n_D(0)$ $\overline{n}_e$ $10^{19}/m^3$		f_{GW}	$T_i(0)/T_e(0)$ keV	β_N	β_p	τ_E^{tot} s	H_{89L}	f_{th}	τ_E^{th} s	H_{98H}	Q_{DT}^{eq}	Δt s	$\Delta t/\tau_E^{tot}$
29941 10.0	1.5	3.7	1.58	0.16	4.0	22.1	4.1	4.1	0.51	8.8 / 4.2	1.68	1.28	0.18	1.61	0.75	0.13	0.90	0.11	8.5	48.6
30006 5.1	1.5	3.6	1.56	0.30	4.5	15.0	4.5	3.1	0.43	11.0 / 6.0	1.98	1.55	0.32	2.33	0.75	0.24	1.18	0.18	4.5	14.3
32218 8.2	1.1	2.1	1.43	0.46	3.3	11.2	2.9	2.6	0.52	8.5 / 5.3	2.68	1.55	0.23	2.15	0.68	0.15	1.02	0.08	2.8	12.4

dW/dt=0, f_{GW}=electron density normalized by Greenwald limit, f_{th}= fraction of thermal component
ripple & orbit loss subtracted (8.8%(E29941),14.8% (E30006), 15.5%(E32218))

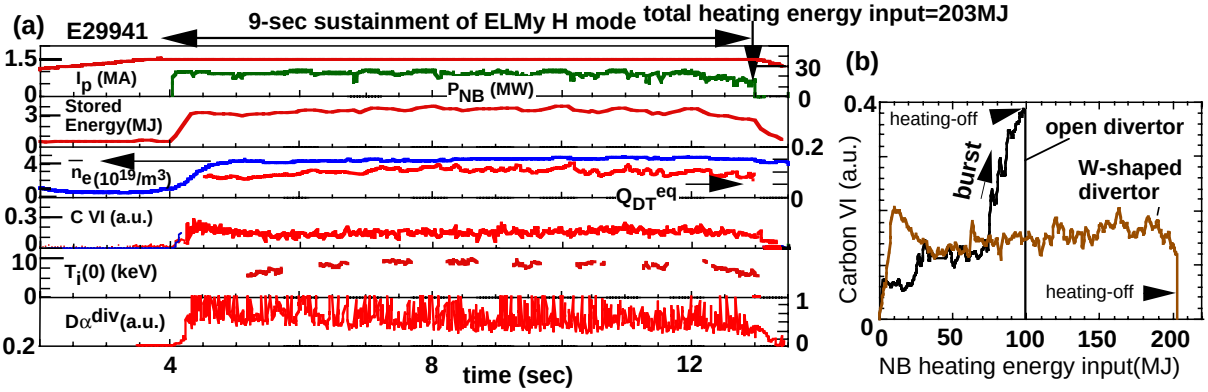

Fig. 2: (a) Evolution of the 9sec-ELMy H-mode. The total NB heating energy reached 203MJ without increase in carbon brightness and particle recycling. (b) With the open divertor, carbon burst was observed at ~70MJ.

(bootstrap ~60%) [1,2]. Recently, with the new W-shaped pumped divertor [3], the high performance discharge regime was extended to the new long-pulse region. The sustained values of the DT equivalent fusion gain Q_{DT}^{eq} and $\beta_N H$ are shown in Fig.1, and the main parameters of the three typical discharges are listed in Table 1. In this paper, the ripple and orbit losses of the injected NB power (~15%) calculated by the OFMC code was subtracted in evaluating the absorbed heating power. The H-factor is defined as the confinement improvement from the ITER-89PL scaling.

As for the longest sustainment (E29941) , the ELMy H-mode with Q_{DT}^{eq}~0.1, H-factor ~1.6, T_i (0)~9keV and β_N~1.7 was sustained for 9 sec (~50τ_E) under a high NB power of 20-25MW (I_p=1.5 MA, B_t=3.6T, δ=0.16) (Fig.2(a)). Since the effective particle confinement time τ_p* was ~ 0.7-0.8s. the sustained duration was sufficiently long compared to the particle confinement (~10 τ_p*). In this discharge, even with the high total energy input up to 203MJ, no increase in impurity (carbon) and

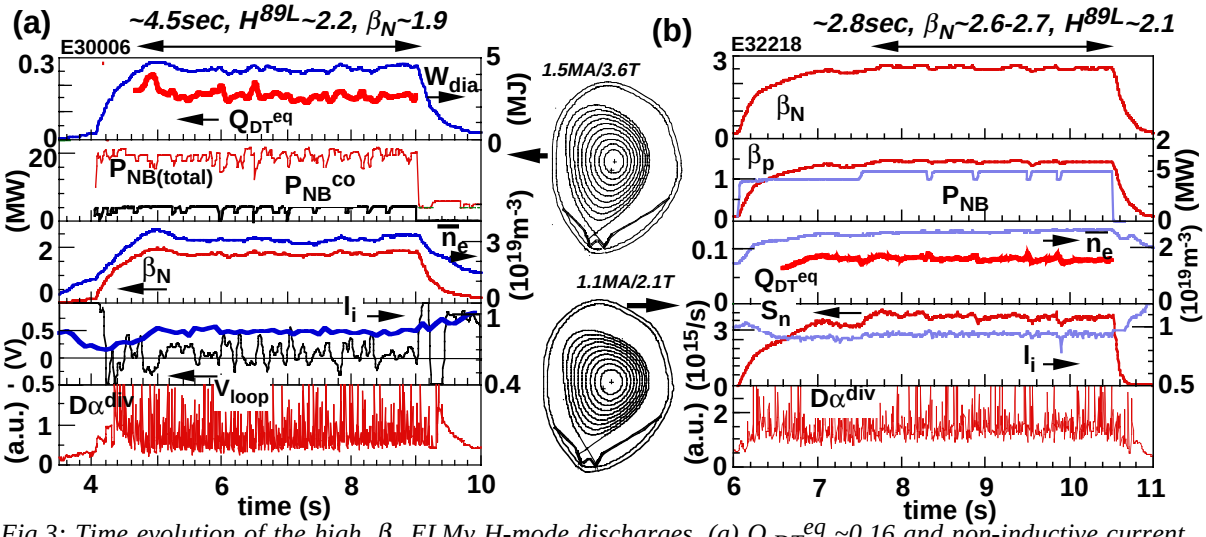

Fig.3: Time evolution of the high β_p ELMy H-mode discharges. (a) Q_{DT}^{eq} ~0.16 and non-inductive current drive fraction ~60-70% were sustained for 4.5s (δ=0.30). (b) β_N ~2.6 was sustained for 2.8s at q_{95}=3.3.

particle recycling was observed. Before the divertor modification, an increase in carbon (Fig.2(b)) and recycling degraded performance at ~3 sec duration of high power (20-30MW) heating (~70-100MJ of the total energy input).

In case of higher δ (=0.3), (Fig.3(a);E30006), the better performance with Q_{DT}^{eq}~0.16, H-factor~ 2.2, β_N~1.9 and β_p~1.6 were sustained for 4.5 s with 60-70% of non-inductive driven current (by ACCOME code) at a relatively high density of ~43% of the Greenwald limit. At δ=0.46 (E32218), a high value of β_N=2.6-2.7 was sustained for 2.8 s at the low value of q_{95}=3.3 (Fig.3(b), see also Fig.6 (b)). In these discharges, the current profile has reached the steady-state in the later phase of the H-mode according to the data of internal inductance and internal poloidal magnetic field by MSE. Duration of the high δ equilibrium is limited (< 5sec) by heat capacity of the shaping coils.

These plasmas with the favorable confinement and stability have been obtained in the high-β_p H-mode [4]. The typical radial profiles at a high δ (=0.49) is given in Fig.4, where, in addition to the edge transport reduction by the H-mode, both χ_i and χ_e drop inside the Internal Transport Barrier (ITB) with the monotonic q-profile (positive magnetic shear). (The time traces of this discharge are given in Fig. 11). In the high-β_p H-mode, although such the double transport barriers are produced for χ_i in a wide range of operation regions, the drop in χ_e at the ITB is not always observed. However, in the high-δ discharges, the drop in χ_e tends to be clearly observed.

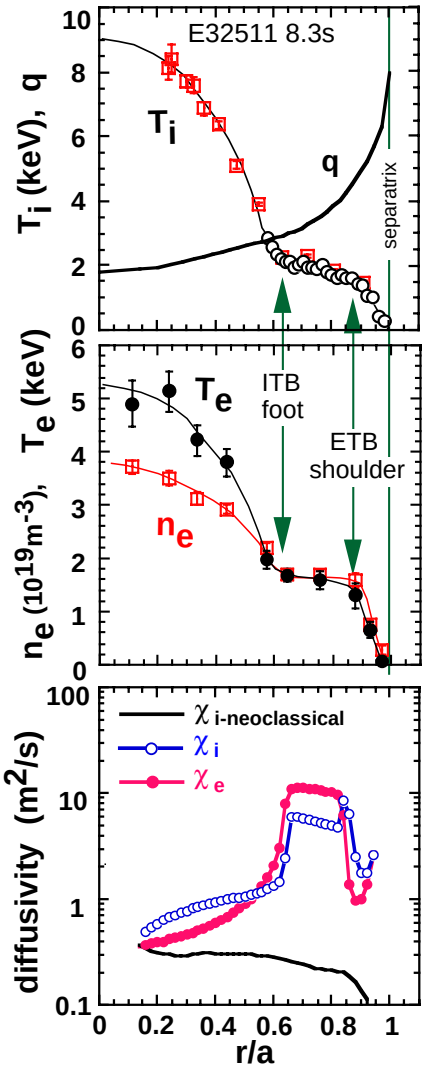

Fig.4 : The typical radial profiles of the high β_p ELMy H-mode at high triangularity δ (=0.49) with the monotonic q-profile. Both χ_i and χ_e drop inside the ITB and in the edge pedestal region.

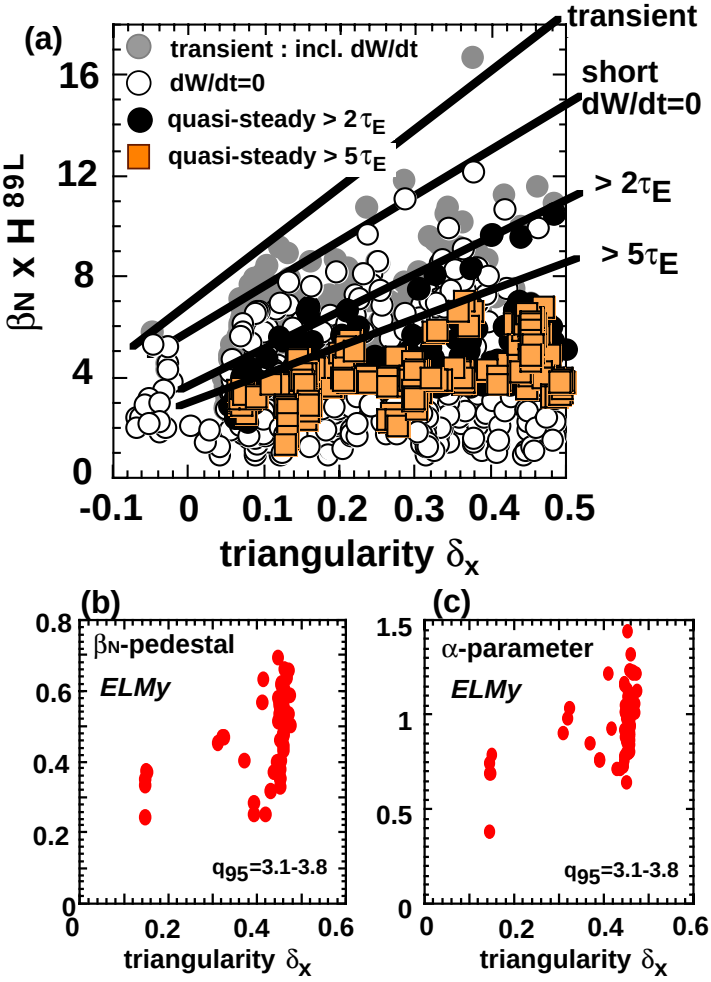

Fig.5: (a) β_N x H-factor increases with triangularity δ (I_p=0.6 - 3.0MA). Sustainable values of $\beta_N H$ for >5 τ_E (~1-2sec) is ~60% of that achievable in a short duration. (b)&(c) The upper limits of the β_N-pedestal and the edge α-parameter increase with δ at fixed q_{95}.

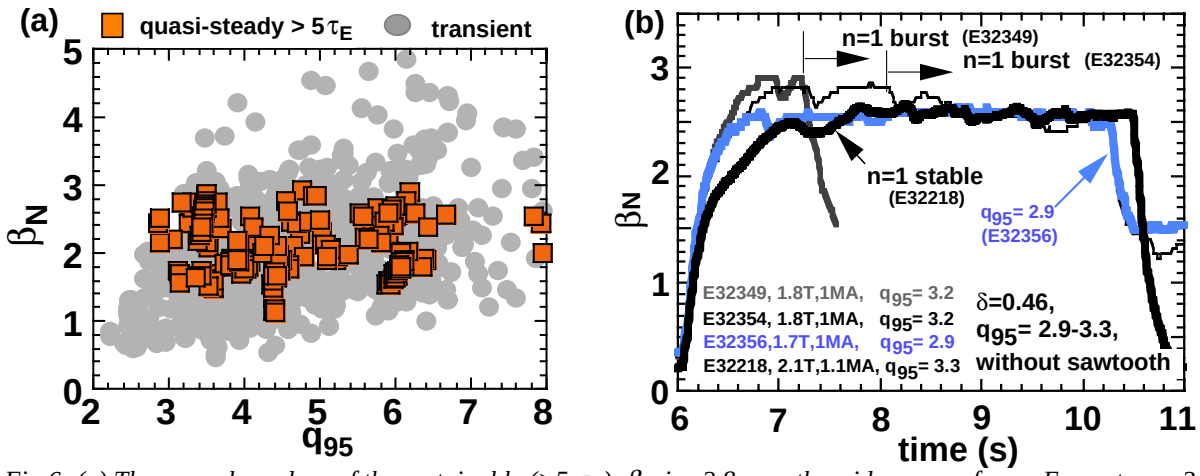

Fig.6: (a) The upper boundary of the sustainable (>5 τ_E) β_N is ~2.8 over the wide range of q_{95}. Even at q_{95}~3, β_N=2.6-2.7 can be sustained. (b) Wave forms of β_N for low-q_{95} (=2.9-3.3) discharges with a high δ (=0.46) and q(0)>1 (no sawtooth). If β_N>2.8, bursts of the n=1 mode degrade the discharge performance.

2. β-LIMITS IN LONG PULSES

In the long pulse discharges, we controlled the heating profile to produce the optimum peakedness of the pressure profile p(r) for maximizing β_N [2]. At a larger peakedness, the β_N-limit is lower due to the β_p-collapse which is consistent with the ideal kink-ballooning limit. At a smaller peakedness, β_N is limited by giant ELMs which is consistent with the high-n ballooning limit. The ELM-limit increases with δ [2]. Figure 5(a) shows β_NH increases with δ in any duration from 'transient' to 'long pulse'. However, the level of β_NH decreases with extending sustainment time. Among discharges with dW/dt=0 (W: stored energy), β_NH decreases by ~40% from the short-duration limit (upper envelope of open circles) to quasi-steady>5τ_E (closed square). One of the main reasons of the better performance at higher-δ is the improved edge pedestal energy caused by the higher limit of the α-parameter (Figs.5 (b) and (c)). As shown later in Fig.9, even in the type-I ELMy phase, the edge plasmas keep a clear and steep gradient structure of the thermal pressure. The pressure gradient is limited by the type-I ELMs (~ high n ideal ballooning mode limit) and the time-averaged pedestal structure seems to be determined by the ELM frequency and heating power. The high δ shape is beneficial to keep the steep pressure gradient inside the pedestal layer.

In a transient phase, the achievable β_N is limited by ideal MHD instabilities. Thus the β_N limit increases with increasing q_{95}, this is because the peakedness of the current profile can be higher (higher l_i) at higher q_{95}. On the other hand, in the long pulse discharges, the upper boundary of the sustainable β_N is ~2.8 over the wide range of q_{95} as shown in Fig.6(a), This limit is due to slowly (~ 100ms) growing resistive instabilities with mode numbers of (m/n)=(3/2), (2/1), (3/1) etc. [2].

Figure 6(a) also shows that β_N ~2.8 can be sustained even in the low-q (q_{95}~3) region. This regime have been newly demonstrated in JT-60U at a high δ. Figure 6(b) shows the traces of β_N for low-q_{95} (=2.9-3.3) discharges with δ=0.46. If β_N>2.8, bursts of the n=1 mode degrade the discharge performance. In this region, the dominant mode number is m/n=2/1. Since these plasmas are the high β_p H-mode with q(0)>1, no sawtooth activity exists. If q(0)<1 in this low-q region, β_N is lower (~ 1.8) due to (m/n)=(1/1) mode and sawteeth [5].

For identification of the slowly growing low-n instabilities, a direct measurement of the evolving island width of the m/n=3/2 mode was carried out [6] by using the heterodyne radiometer with a fine spatial resolution of ~2cm in the radial direction. This mode number m/n=3/2 is often observed in long-pulse discharges at q_{95}~3.5 - 4.5. Figure 7(a) shows the electron temperature profiles T_e(r) both when the line of sight of the measurement is looking at the O-point and the X-point of the rotating magnetic island. (Note: These T_e(r) are the partial profiles from R= 3.5 to 3.8m just around the island region). From the O-point measurement, the island width can be evaluated as ~ 7cm. Figures 7(b) and(c) show that the island width increases with the magnetic fluctuation. In this discharge, the

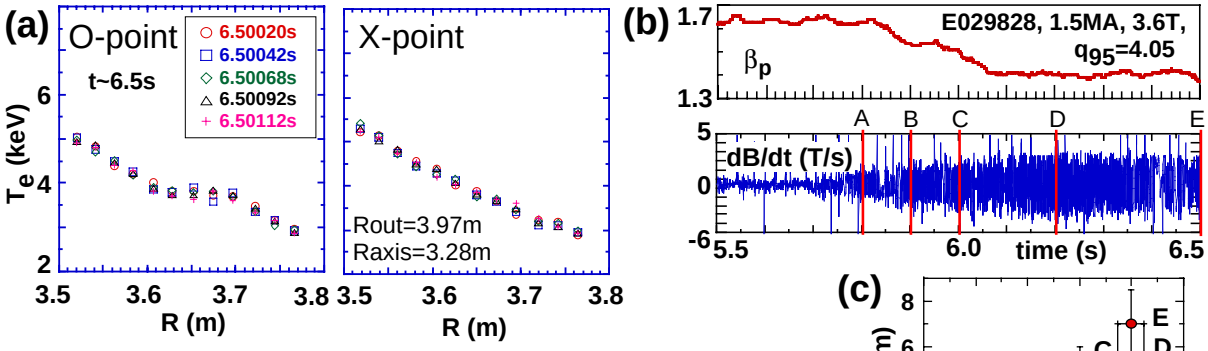

Fig.7: (a) The magnetic island width of the m/n=3/2 mode was measured by the heterodyne radiometer. The island width increases with the magnetic fluctuation (b)&(c) and the saturated value is ~ 7 cm.

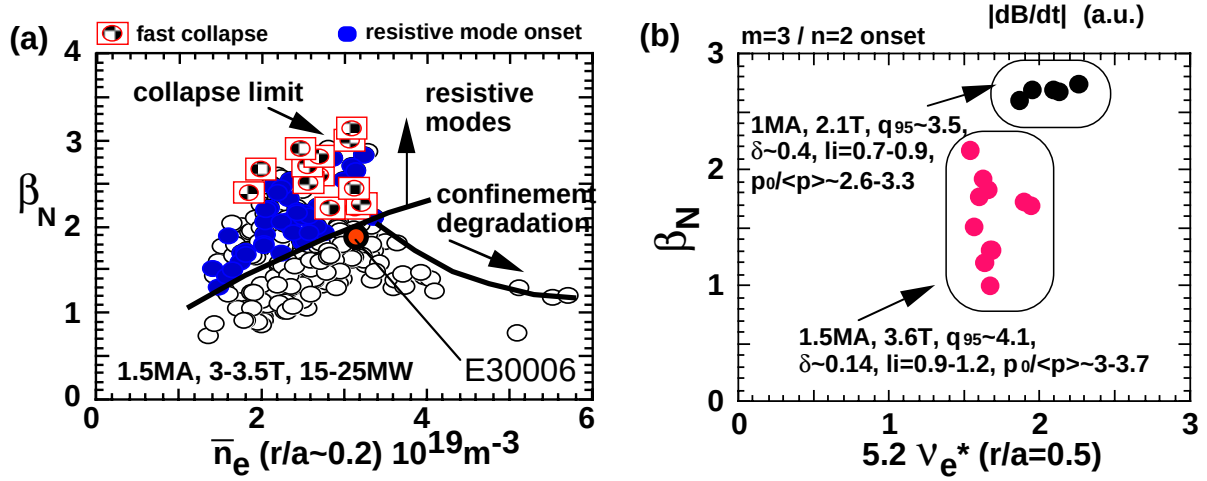

Fig.8: (a) Regions of fast collapses, onset of resistive modes and degradation in confinement on the $\bar{n}_e$ - β_N plane (I_p=1.5MA, B_t=3-3.5T, δ<0.3, P_{NB}=15-25MW). The lower boundary of the resistive mode increases with $\bar{n}_e$. (b) The β_N value at the m/n=3/2 mode onset does not show a clear dependence on collisionality evaluated at r=a/2.

saturated value of the island width is ~ 7 cm. This island width agrees with the theoretically predicted width [7] of ~9cm for the neoclassical tearing mode [6].

The threshold β_N for onset of the resistive modes increases with increasing electron density and with broadening of p(r). Figure 8(a) shows the density dependence at I_p=1.5MA, B_t=3-3.5T and δ<0.3 where the closed circles correspond to onset of the resistive modes. In this figure, at a density higher than ~3.4×10^{19}m^{-3} (~50% of Greenwald limit), β_N decreases because of confinement degradation by high recycling. For sustainment of the long pulse discharges, we kept the optimum set of density and β_N to avoid both the resistive modes and confinement degradation. (For example, the shot E30006 shown in Fig.3(a) has β_N =2 with $\bar{n}_e$=3.2×10^{19}m^{-3}.) In Fig.8(a), the threshold β_N for the resistive mode increases with density. However, no clear tendency of the threshold value related to the collisionality [8] has been observed in JT-60U as shown in Fig.8(b). Increase in density tends to broaden the pressure profile. This effect changes the local combination of the pressure and the current profiles and, thus, the stability can be affected. The JT-60U data suggest a broader pressure profile tends to be more stable against the m/n=3/2 mode.

3. EDGE PEDESTAL EVOLUTION IN THE ELMy H-MODE

To sustain high confinement, control of the edge pedestal structure is essential. In JT-60U ELM-free H-mode, the edge pedestal width Δ-ped is 3-5cm at I_p~2MA and scales roughly with the ion poloidal gyro radius [9]. On the other hand, in the giant-ELMy phase, Δ-ped can be 10-15cm (r/a~80 %). Figure 9(a) shows a typical ELMy discharge at I_p=1MA, q_{95}=3.5 and δ=0.46, where the type I

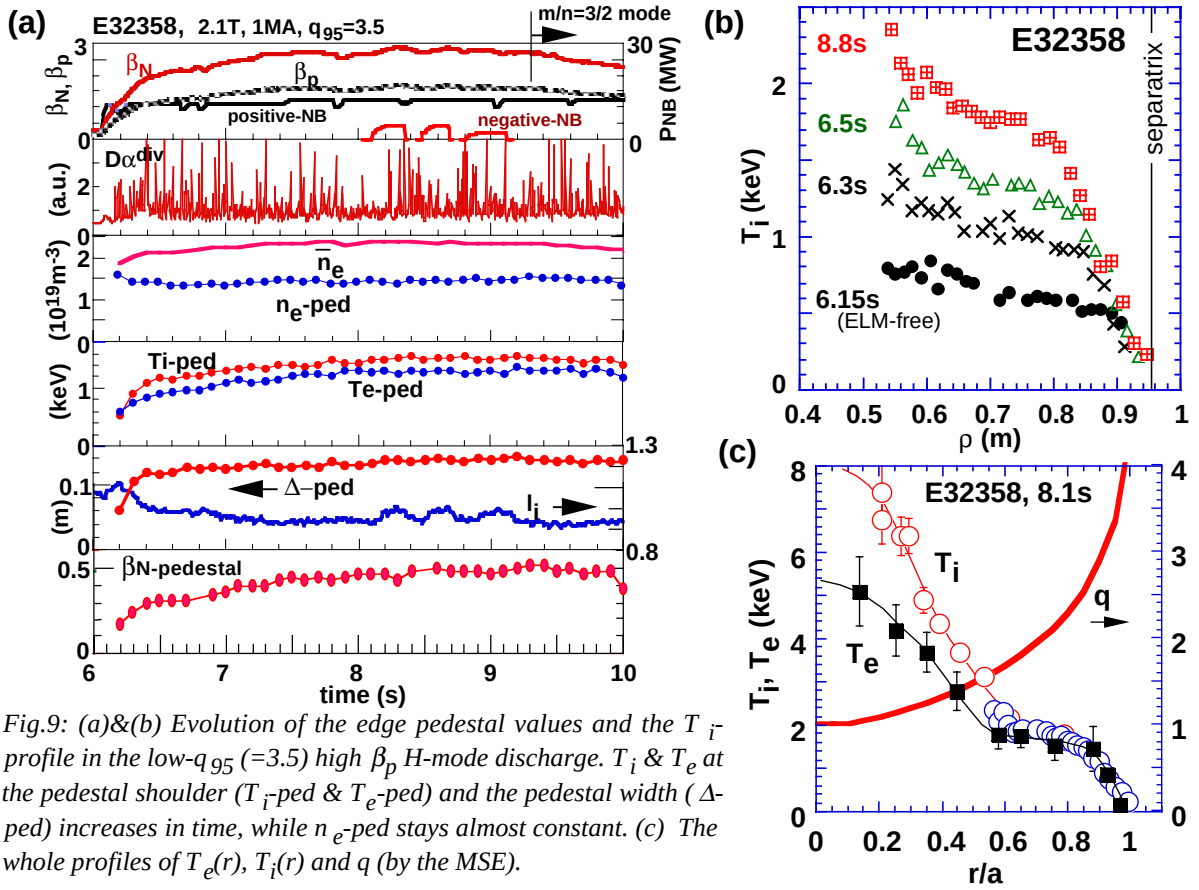

Fig.9: (a)&(b) Evolution of the edge pedestal values and the T_i-profile in the low-q_{95} (=3.5) high β_p H-mode discharge. T_i & T_e at the pedestal shoulder (T_i-ped & T_e-ped) and the pedestal width (Δ-ped) increases in time, while n_e-ped stays almost constant. (c) The whole profiles of $T_e(r)$, $T_i(r)$ and q (by the MSE).

ELMs (giant ELMs) are observed throughout the NB heating phase. The time evolution of the ion temperature profile $T_i(r)$ is given in Fig.9(b) and the time evolution of T_i-ped, T_e-ped, n_e-ped and Δ-ped are shown in Fig.9(a). In the ELM-free phase (t~6.15s), both T_i-ped (T_i at the pedestal shoulder) and the pedestal depth Δ-ped are small. In the ELMy phase, these parameters increase gradually in time. Here, T_i was measured by the CXR system with the time resolution of 50ms. Since the ELM frequency of the discharge is 50 - 100 Hz, the measured $T_i(r)$ is the time-averaged profile over a few ELMs. The profiles of T_e and n_e were measured by the YAG Thomson scattering system with the measuring time of 20ns. Therefore, the measured values of T_e and n_e in the pedestal layer is affected

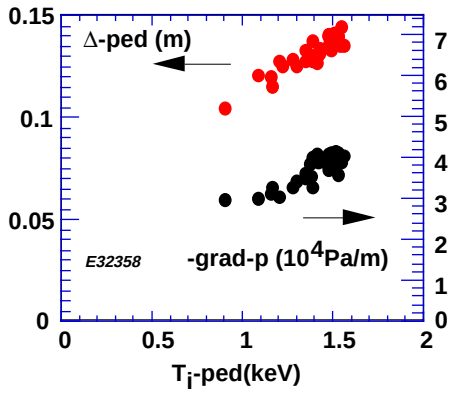

Fig.10: Δ-ped and the edge pressure gradient increases with T_i-ped (E32358).

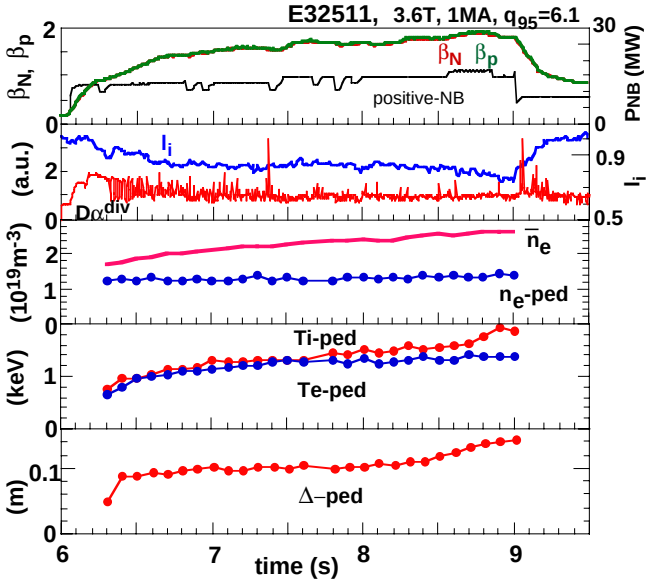

Fig.11: Evolution of the edge pedestal values in the high-q_{95} (=6.1) high β_p H-mode discharge. The ELM activity disappears (t ~ 8 - 9s) and Δ-ped and T_i-ped increase further. (For profiles, see Fig.4)

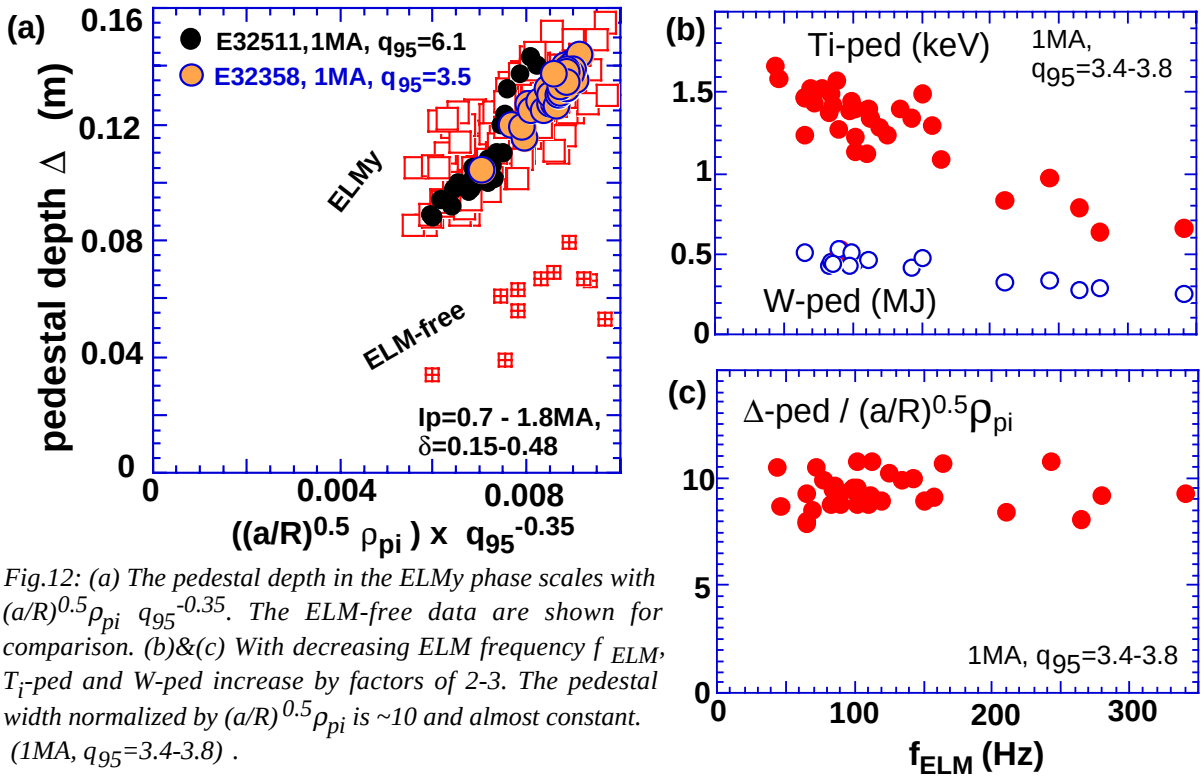

Fig.12: (a) The pedestal depth in the ELMy phase scales with $(a/R)^{0.5}\rho_{pi}\ q_{95}^{-0.35}$. *The ELM-free data are shown for comparison. (b)&(c) With decreasing ELM frequency* f_{ELM}, T_i*-ped and W-ped increase by factors of 2-3. The pedestal width normalized by* $(a/R)^{0.5}\rho_{pi}$ *is ~10 and almost constant. (1MA,* q_{95}*=3.4-3.8) .*

by the relative timing of an ELM and the Thomson laser launch. On the other hand, T_e and n_e in the inner area does not seem to be affected very much. Therefore, For the evaluation of T_e-ped and n_e-ped, we excluded the data just during the ELM burst of D_α brightness and, in addition, we used the fitting of the inner data and did not use the data inside the pedestal layer. In Fig.9(a), T_i-ped, T_e-ped and Δ-ped increases in time, while n_e-ped stays almost constant. The time scale of the pedestal evolution is gradual (~2s) and much longer than τ_E (~ 0.2s). Figure 10 shows that Δ-ped and the edge pressure gradient increase with T_i-ped. On the other hand, at high-q_{95} (=6.1; I_p=1MA, δ=0.49), the behavior of ELMs are different. Figure 11 shows that the ELM activity is weaker than that in the low-q_{95} discharge in Fig.9. In particular, the ELM activity disappears at t ~8 -9s, and Δ-ped and T_i-ped increase further. The internal inductance l_i decreases almost simultaneously. Such disappearance of ELMs are observed when δ>0.3-0.4, β_p>1.5-2.0 and q_{95}>5-6. In this parameter region, the minute grassy ELMs are observed when I_p is smaller (typically ~0.6MA) [2,10]. It seems that the increase in Δ-ped and T_i-ped coincide with disappearance of the ELMs. The access to the second stability regime for the high n ballooning mode may cause this phenomena.

The width Δ-ped in the ELMy phase scales with $(a/R)^{0.5}\rho_{pi}\ q_{95}^{-0.35}$ (Fig.12(a)), where evolution of E32511(Fig.11) and E32358 (Fig.9) are shown by closed circles. The q-dependence, not strong, was evaluated from these two cases. For a fixed q_{95} ~3-4, Δ-ped is proportional to $\sim 10(a/R)^{0.5}\rho_{pi}$ and is 2 -3 times larger than that of the ELM-free phase. (In the figure, the ELM-free data are shown just for comparison. For the ELM-free data, no q-dependence has been observed [9].) The ELM frequency f_{ELM} is an important parameter for the development of the pedestal structure. Figure 12(b) shows that T_i-ped and W-ped increase by factor of 2-3 with decreasing f_{ELM}. On the other hand, the normalized width Δ-ped/$((a/R)^{0.5}\rho_{pi})$ is ~10 and almost constant over the wide range of f_{ELM}. (1MA, q_{95}=3.4-3.8). The pedestal width seems to be determined by both MHD stability (ELM) and transport related to ρ_{pi}. This combined effect on the pedestal structure formation in the ELMy phase is to be understood for optimizing the integrated performance including SOL and divertor plasmas.

4. SUMMARY

The JT-60U discharge regions toward the steady-state high integrated performance are summarized in Fig.13. Before the divertor modification, we mainly focused on the concept

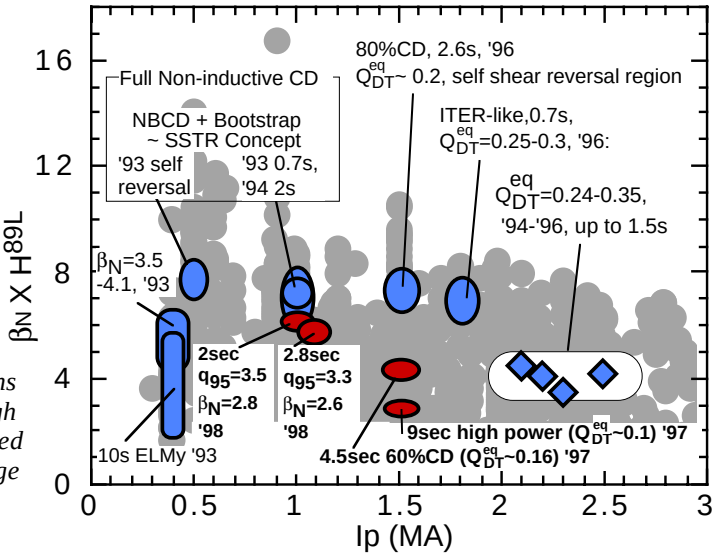

Fig.13:
Summary for the JT-60U discharge regions of ELMy quasi-steady discharges with high integrated performances. The shadowed back ground shows the whole discharge region including transient data.

optimization of the ELMy plasmas with high integrated performance [1,2]. After the modification to the new W-shaped pumped divertor, we have been focusing on i) long sustainment time,ii) increase in absolute values of fusion performance and iii) expansion of the discharge regime toward low-q (q_{95}~3). A long heating time with a high total heating energy input of 203MJ became possible without harmful increase in impurity and particle recycling. In addition, optimization of p(r) with the double transport barriers, n_e and / or high δ enabled us to extend the long-pulse performances; Q_{DT}^{eq}~0.1 (δ =0.16) was sustained for ~9 sec (~50τ_E, ~10τ_p*) and Q_{DT}^{eq}~0.16 for 4.5 sec (δ = 0.3) at I_p=1.5MA. In the latter case, H-factor ~2.2 and β_N~1.9 were sustained with 60-70% of noninductive driven current. The sustainable value of $\beta_N H$ increases with increasing δ. In the region of low q_{95} (~3), the high-β stability was improved by the high δ (~ 0.46) shape where β_N~2.5-2.7 was sustained for ~3.5s with the collisionality close to that of ITER-FDR plasmas. These long pulses have made progress in studies on the key physics issues for the steady-state tokamak operation: The sustainable β_N is limited by the low-n resistive modes. The direct measurement of the island width shows the agreement with the neoclassical tearing mode theory. However, no clear effects by collisionality was observed. The edge pedestal width Δ-ped evolves gradually (~2 s) with increasing T_i-ped and the saturated width (10-15cm at I_p=1MA) is 2-3 times larger than that in the ELM-free phase. The data shows that Δ-ped is proportional to $(a/R)^{0.5}\rho_{pi}$. The edge α-parameter increases with increasing δ, which is the main reason of the improved high-β stability in a long pulse by high-δ.

ACKNOWLEDGMENTS

The authors would like to thank the members of JAERI who have contributed to the JT-60U project.

REFERENCES

[1] KAMADA, Y., et al., Plasma Phys. Cont. Nucl. Fusion Res. Proc.15th Int. Conf. (Seville, 1994) Vol 1, p651.
[2] KAMADA, Y., et al., Fusion Energy Proc. 16th Int. Conf. (Montreal, 1996) Vol 1, p247.
[3] HOSOGANE, N., et al., Fusion Energy Proc. 16th Int. Conf. (Montreal, 1996) GP-11.
[4] MORI, M ., et al., Nucl. Fusion 34 (1994) 1405.
[5] ISHIDA , S., et al., Fusion Energy Proc. 16th Int. Conf. (Montreal, 1996) Vol 1, p315.
[6] ISAYAMA, A., et al., submitted to Plasma Phys. Control. Fusion.
[7] FITZPATRICK, R., Phys. Plasmas 2 (1995) 825.
[8] SAUTE, O., et al., Phys. Plasmas 4 (1997) 1654.
[9] HATAE, T., et al., Plasma Phys. Control. Fusion 40 (1998) 1073.
[10] KAMADA, Y., Plasma Phys. Control. Fusion 38 (1996) 1387.